

The inverse thermal spin-orbit torque and the relation of the Dzyaloshinskii-Moriya interaction to ground-state energy currents

Frank Freimuth, Stefan Blügel and Yuriy Mokrousov

Peter Grünberg Institut and Institute for Advanced Simulation, Forschungszentrum Jülich and JARA, 52425 Jülich, Germany

E-mail: f.freimuth@fz-juelich.de

Abstract. Using the Kubo linear-response formalism we derive expressions to calculate the heat current generated by magnetization dynamics in magnets with broken inversion symmetry and spin-orbit interaction (SOI). The effect of producing heat currents by magnetization dynamics constitutes the Onsager reciprocal of the thermal spin-orbit torque (TSOT), i.e., the generation of torques on the magnetization due to temperature gradients. We find that the energy current driven by magnetization dynamics contains a contribution from the Dzyaloshinskii-Moriya interaction (DMI), which needs to be subtracted from the Kubo linear response of the energy current in order to extract the heat current. We show that the expressions of the DMI coefficient can be derived elegantly from the DMI energy current. Guided by formal analogies between the Berry phase theory of DMI on the one hand and the modern theory of orbital magnetization on the other hand we are led to an interpretation of the latter in terms of energy currents as well. Based on *ab-initio* calculations we investigate the heat current driven by magnetization dynamics in Mn/W(001) magnetic bilayers. We predict that fast domain walls drive strong ITSOT heat currents.

PACS numbers: 72.25.Ba, 72.25.Mk, 71.70.Ej, 75.70.Tj

1. Introduction

The interaction of heat current with electron spins is at the heart of spin caloritronics [1]. It leads to thermal spin-transfer torques (STTs) on the magnetization in spin valves, magnetic tunnel junctions, and domain walls when a temperature gradient is applied [2, 3, 4, 5, 6, 7, 8]. While the thermal STT does not require spin-orbit interaction (SOI), it only exists in noncollinear magnets. In spin valves and magnetic tunnel junctions this noncollinearity arises when the magnetizations of the free and fixed layers are not parallel, while in domain walls it arises from the continuous rotation of magnetization across the wall.

In the presence of SOI electric currents and heat currents can generate torques also in collinear magnets: In ferromagnets with broken inversion symmetry the so-called spin-orbit torque (SOT) acts on the magnetization when an electric current is applied (Figure 1a) [9, 10, 11, 12, 13, 14, 15, 16, 17]. The inverse spin-orbit torque (ISOT) consists in the production of an electric current due to magnetization dynamics (Figure 1b) [18, 19, 20]. The application of a temperature gradient results in the thermal spin-orbit torque (TSOT) (Figure 1c) [21]. TSOT and SOT are related by a Mott-like expression [22].

In this work we discuss the inverse effect of TSOT, i.e., the generation of heat current due to magnetization dynamics in ferromagnets with broken inversion symmetry and SOI (Figure 1d). We refer to this effect as inverse thermal spin-orbit torque (ITSOT). While the SOT is given directly by the linear response of the torque to an applied electric field [16], expressions for the ITSOT are more difficult to derive because the energy current obtained from the Kubo formalism contains also a ground-state contribution that does not contribute to the heat current. Analogous difficulties are known from the case of the inverse anomalous Nernst effect, i.e., the generation of a heat current transverse to an applied electric field \mathbf{E} [23]. In this case the energy current obtained from the Kubo formalism contains besides the heat current also the material-dependent part $-\mathbf{E} \times \mathbf{M}^{\text{orb}}$ of the Poynting vector, where \mathbf{M}^{orb} is the orbital magnetization. This energy magnetization does not contribute to the heat current and needs to be subtracted from the Kubo linear response [23, 24, 25].

When inversion symmetry is broken in magnets with SOI the expansion of the free energy F in terms of the magnetization direction $\hat{\mathbf{n}}(\mathbf{r})$ and its gradients contains a term linear in the gradients of magnetization, the so-called Dzyaloshinskii-Moriya interaction (DMI) [26, 27]:

$$F^{\text{DMI}}(\mathbf{r}) = \sum_j \mathbf{D}_j(\hat{\mathbf{n}}(\mathbf{r})) \cdot \left(\hat{\mathbf{n}}(\mathbf{r}) \times \frac{\partial \hat{\mathbf{n}}(\mathbf{r})}{\partial r_j} \right), \quad (1)$$

where \mathbf{r} is the position and the index j runs over the three cartesian directions, i.e., $r_1 = x, r_2 = y, r_3 = z$. The DMI coefficients \mathbf{D}_j can be expressed in terms of mixed Berry phases [22, 28]. DMI does not only affect the magnetic structure by energetically favoring spirals of a certain handedness but also enters spin caloritronics effects [29, 30]. Here, we will show that DMI gives rise to the ground-state energy current

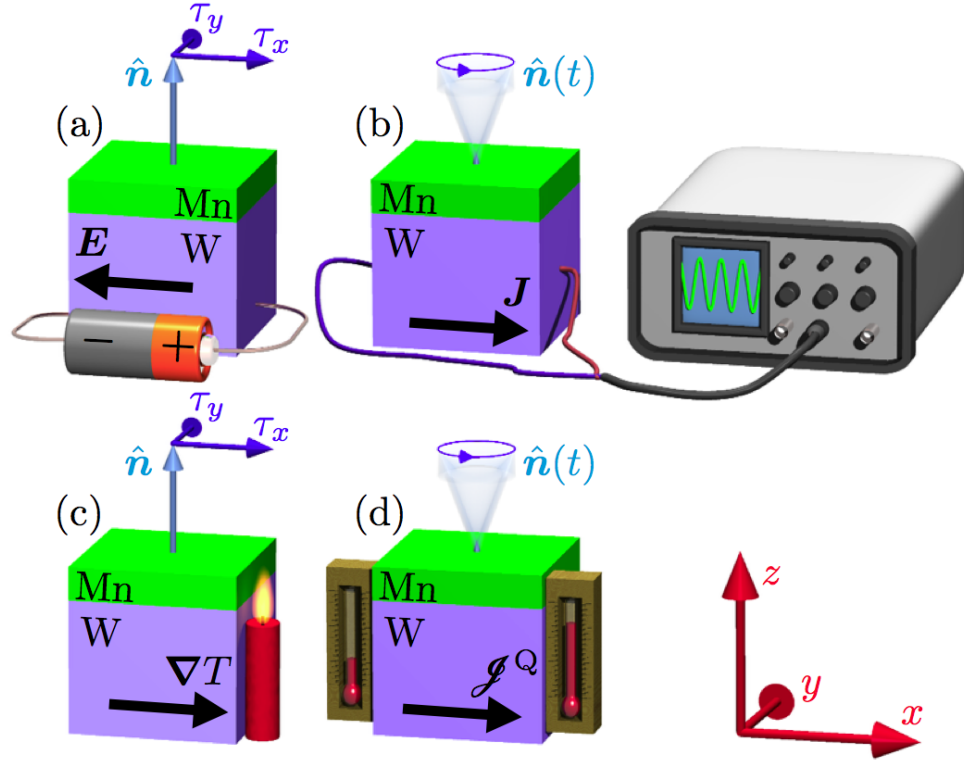


Figure 1. Family of SOT-related effects in a Mn/W magnetic bilayer with broken structural inversion symmetry. (a) SOT: An applied electric field \mathbf{E} generates a torque $\boldsymbol{\tau}$ on the magnetization. $\hat{\mathbf{n}}$ is the magnetization direction. (b) ISOT: Magnetization dynamics $\partial \hat{\mathbf{n}} / \partial t$ drives an electric current \mathbf{J} . (c) TSOT: The application of a temperature gradient ∇T generates a torque $\boldsymbol{\tau}$. (d) ITSOT: Magnetization dynamics drives a heat current \mathcal{J}^Q .

$\mathcal{J}_j^{\text{DMI}} = -\mathbf{D}_j \cdot (\hat{\mathbf{n}} \times \frac{\partial \hat{\mathbf{n}}}{\partial t})$ when magnetization precesses. This DMI energy current needs to be subtracted from the linear response of the energy current in order to obtain the ITSOT heat current.

This work is structured as follows. In section 2 we show that magnetization dynamics drives a ground-state energy current associated with DMI and we highlight its formal similarities with the material-dependent part of the Poynting vector. In section 3 we develop the theory of ITSOT. We derive the energy current based on the Kubo linear-response formalism and subtract \mathcal{J}^{DMI} in order to extract the heat current. In section 4 we show that the expressions of DMI and orbital magnetization can also be derived elegantly by equating the energy currents obtained from linear response theory to \mathcal{J}^{DMI} and $-\mathbf{E} \times \mathbf{M}^{\text{orb}}$, respectively. In section 5 we present *ab-initio* calculations of TSOT and ITSOT in Mn/W(001) magnetic bilayers.

2. Ground-state energy current associated with the Dzyaloshinskii-Moriya interaction

To be concrete, we consider a flat cycloidal spin spiral propagating along the x direction. The magnetization direction is given by

$$\hat{\mathbf{n}}_c(\mathbf{r}) = \hat{\mathbf{n}}_c(x) = \begin{pmatrix} \sin(qx) \\ 0 \\ \cos(qx) \end{pmatrix}, \quad (2)$$

where q is the spin-spiral wavenumber, i.e., the inverse wavelength of the spin spiral multiplied by 2π . The free energy contribution $F^{\text{DMI}}(\mathbf{r})$ given in (1) simplifies for the spin spiral of (2) as follows:

$$\begin{aligned} F^{\text{DMI}}(\mathbf{r}) &= F^{\text{DMI}}(x) = \mathbf{D}_x(\hat{\mathbf{n}}_c(x)) \cdot \left[\hat{\mathbf{n}}_c(x) \times \frac{\partial \hat{\mathbf{n}}_c(x)}{\partial x} \right] = \\ &= q \mathbf{D}_x(\hat{\mathbf{n}}_c(x)) \cdot \hat{\mathbf{e}}_y = q \mathcal{D}_{xy}(\hat{\mathbf{n}}_c(x)), \end{aligned} \quad (3)$$

where $\hat{\mathbf{e}}_y$ is the unit vector pointing in y direction and we defined $\mathcal{D}_{ij}(\hat{\mathbf{n}}) = \mathbf{D}_i(\hat{\mathbf{n}}) \cdot \hat{\mathbf{e}}_j$. Whether \mathcal{D}_{xy} is nonzero or not depends on crystal symmetry. The tensor $\mathcal{D}_{ij}(\hat{\mathbf{n}})$ is axial and of second rank like the SOT torque tensor [22]. Additionally, it is even under magnetization reversal, i.e., $\mathcal{D}_{ij}(\hat{\mathbf{n}}) = \mathcal{D}_{ij}(-\hat{\mathbf{n}})$. Therefore, $\mathcal{D}_{ij}(\hat{\mathbf{n}})$ has the same symmetry properties as the even SOT torque tensor [16]. According to (3) the cycloidal spiral of (2) is affected by DMI if \mathcal{D}_{xy} is nonzero. This is the case e.g. for magnetic bilayers such as Mn/W(001) and Co/Pt(111) (the interface normal points in z direction), where also the component t_{yx} of the even SOT torque tensor is nonzero [16, 22, 31, 32].

We consider now a Neel-type domain wall that moves with velocity $w < 0$ in x direction. The magnetization direction at time $t_0 = 0$, which we denote by $\hat{\mathbf{n}}_0(x)$, is illustrated in Figure 2a. $\hat{\mathbf{n}}_0(x)$ can be interpreted as a modification of $\hat{\mathbf{n}}_c(x)$ ((2)), where the q -vector depends on position:

$$\hat{\mathbf{n}}_0(x) = \begin{pmatrix} \sin(q(x)x) \\ 0 \\ \cos(q(x)x) \end{pmatrix}. \quad (4)$$

Since the domain wall moves with velocity w , the magnetization direction $\hat{\mathbf{n}}(x, t)$ at position x and time t is given by

$$\hat{\mathbf{n}}(x, t) = \hat{\mathbf{n}}_0(x - wt). \quad (5)$$

In Figure 2 we discuss the magnetization direction at position x_0 at the three times $t_0 = 0$, $t_1 > t_0$ and $t_2 > t_1$. At time $t_0 = 0$ the domain wall is far away from x_0 . Therefore, the magnetization is collinear at x_0 and $F^{\text{DMI}}(x_0, t_0) = 0$. At time t_1 the domain wall starts to arrive at x_0 . Consequently, the magnetization gradient $\partial \hat{\mathbf{n}}(x_0, t_1) / \partial x_0$ becomes nonzero and thus $F^{\text{DMI}}(x_0, t_1) \neq 0$. Due to the motion of the

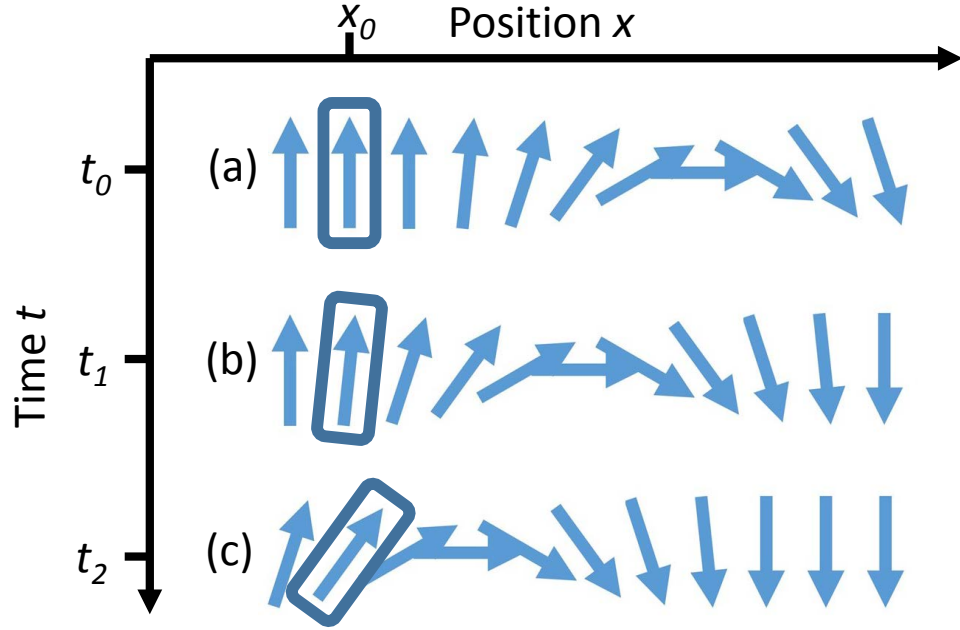


Figure 2. Illustration of a Neel-type domain wall that moves into the negative x direction. Arrows represent the magnetization direction $\hat{\mathbf{n}}(x, t)$. $\hat{\mathbf{n}}(x_0, t)$ is highlighted by oval boxes. (a) $\hat{\mathbf{n}}(x, t_0) = \hat{\mathbf{n}}_0(x)$ is locally collinear at x_0 and therefore $F^{\text{DMI}}(x_0, t_0) = 0$. (b) $\hat{\mathbf{n}}(x, t_1) = \hat{\mathbf{n}}_0(x - wt_1)$ starts to become noncollinear at x_0 and therefore $F^{\text{DMI}}(x_0, t_1) \neq 0$. (c) $\hat{\mathbf{n}}(x, t_2)$ is strongly noncollinear at x_0 .

domain wall the DMI contribution $F^{\text{DMI}}(x, t)$ to the free energy is time dependent: How much DMI free energy is stored at a given position in the magnetic structure is determined by the local gradient of magnetization, which moves together with the magnetic structure. The partial derivative of $F^{\text{DMI}}(x, t)$ with respect to time is given by

$$\begin{aligned}
\frac{\partial F^{\text{DMI}}(x, t)}{\partial t} &= \\
&= \mathbf{D}_x(\hat{\mathbf{n}}_0(x - wt)) \cdot \left[\hat{\mathbf{n}}_0(x - wt) \times \frac{\partial^2 \hat{\mathbf{n}}_0(x - wt)}{\partial x \partial t} \right] + \\
&\quad + \frac{\partial \mathbf{D}_x(\hat{\mathbf{n}}_0(x - wt))}{\partial t} \cdot \left[\hat{\mathbf{n}}_0(x - wt) \times \frac{\partial \hat{\mathbf{n}}_0(x - wt)}{\partial x} \right] = \\
&= \mathbf{D}_x(\hat{\mathbf{n}}_0(x - wt)) \cdot \left[\hat{\mathbf{n}}_0(x - wt) \times \frac{\partial^2 \hat{\mathbf{n}}_0(x - wt)}{\partial x \partial t} \right] + \\
&\quad + \frac{\partial \mathbf{D}_x(\hat{\mathbf{n}}_0(x - wt))}{\partial x} \cdot \left[\hat{\mathbf{n}}_0(x - wt) \times \frac{\partial \hat{\mathbf{n}}_0(x - wt)}{\partial t} \right] = \\
&= \frac{\partial}{\partial x} \left\{ \mathbf{D}_x(\hat{\mathbf{n}}_0(x - wt)) \cdot \left[\hat{\mathbf{n}}_0(x - wt) \times \frac{\partial \hat{\mathbf{n}}_0(x - wt)}{\partial t} \right] \right\} = \\
&= -\frac{\partial}{\partial x} \mathcal{J}_x^{\text{DMI}},
\end{aligned} \tag{6}$$

where $\mathcal{J}_x^{\text{DMI}}$ in the last line is the x component of the DMI energy current density

$$\begin{aligned}\mathcal{J}^{\text{DMI}} &= - \sum_{ij} \hat{\mathbf{e}}_j \mathcal{D}_{ji}(\hat{\mathbf{n}}) \left[\hat{\mathbf{e}}_i \cdot \left(\hat{\mathbf{n}} \times \frac{\partial \hat{\mathbf{n}}}{\partial t} \right) \right] \\ &= - \mathcal{D}(\hat{\mathbf{n}}) \left(\hat{\mathbf{n}} \times \frac{\partial \hat{\mathbf{n}}}{\partial t} \right).\end{aligned}\tag{7}$$

By considering additionally spirals propagating in y and z direction we find that the general form of (6) is the continuity equation

$$\frac{\partial F^{\text{DMI}}}{\partial t} + \nabla \cdot \mathcal{J}^{\text{DMI}} = 0\tag{8}$$

of the DMI energy current \mathcal{J}^{DMI} . According to (7) and (8) the energy current \mathcal{J}^{DMI} is driven by magnetization dynamics and its sources and sinks signal the respective decrease and increase of DMI energy density. When we compute the energy current driven by magnetization dynamics in section 3 we therefore need to be aware that this energy current contains \mathcal{J}^{DMI} in addition to the ITSOT heat current that we wish to determine. Thus, we need to subtract \mathcal{J}^{DMI} from the energy current in order to extract the ITSOT heat current.

It is reassuring to verify that the material-dependent part $\mathcal{J}^{\text{orb}} = -\mathbf{E} \times \mathbf{M}^{\text{orb}}$ of the Poynting vector, which needs to be subtracted from the energy current to obtain the heat current in the case of the inverse anomalous Nernst effect [23], can be identified by arguments analogous to the above. We sketch this in the following. The energy density due to the interaction between orbital magnetization \mathbf{M}^{orb} and magnetic field \mathbf{B} is given by

$$F^{\text{orb}}(\mathbf{r}, t) = -\mathbf{M}^{\text{orb}}(\mathbf{r}, t) \cdot \mathbf{B}(\mathbf{r}, t).\tag{9}$$

We assume that the magnetic field is of the form

$$\mathbf{B}(\mathbf{r}, t) = B_0(x - wt)\hat{\mathbf{e}}_z,\tag{10}$$

i.e., the magnetic field at time t can be obtained from the magnetic field at time $t_0 = 0$ by shifting it by wt , as illustrated in Figure 3. Additionally, we assume that the orbital magnetization is of the same form, i.e., $\mathbf{M}^{\text{orb}}(\mathbf{r}, t) = M_0^{\text{orb}}(x - wt)\hat{\mathbf{e}}_z$. Consequently, also $F^{\text{orb}}(\mathbf{r}, t) = F_0^{\text{orb}}(x - wt)$. $\mathbf{B}(\mathbf{r}, t)$ can be expressed as $\mathbf{B}(\mathbf{r}, t) = \nabla \times \mathbf{A}(\mathbf{r}, t)$ in terms of the vector potential

$$\mathbf{A}(\mathbf{r}, t) = \hat{\mathbf{e}}_y \int_0^{x-wt} B_0(x') dx'.\tag{11}$$

Due to the motion of the profile of $\mathbf{B}(\mathbf{r}, t)$ the energy density in (9) changes as a function

of time. The partial derivative of $F^{\text{orb}}(\mathbf{r}, t)$ with respect to time is

$$\begin{aligned}
\frac{\partial F^{\text{orb}}}{\partial t} &= -\frac{\partial \mathbf{M}^{\text{orb}}}{\partial t} \cdot \mathbf{B} - \mathbf{M}^{\text{orb}} \cdot \frac{\partial \mathbf{B}}{\partial t} \\
&= w \frac{\partial \mathbf{M}^{\text{orb}}}{\partial x} \cdot [\nabla \times \mathbf{A}] + \mathbf{M}^{\text{orb}} \cdot [\nabla \times \mathbf{E}] \\
&= w \frac{\partial \mathbf{M}^{\text{orb}}}{\partial x} \cdot \hat{\mathbf{e}}_z \frac{\partial A_y}{\partial x} + \mathbf{M}^{\text{orb}} \cdot [\nabla \times \mathbf{E}] \\
&= -\frac{\partial \mathbf{M}^{\text{orb}}}{\partial x} \cdot \hat{\mathbf{e}}_z \frac{\partial A_y}{\partial t} + \mathbf{M}^{\text{orb}} \cdot [\nabla \times \mathbf{E}] \\
&= -\mathbf{E} \cdot [\nabla \times \mathbf{M}^{\text{orb}}] + \mathbf{M}^{\text{orb}} \cdot [\nabla \times \mathbf{E}] \\
&= \nabla \cdot [\mathbf{E} \times \mathbf{M}^{\text{orb}}],
\end{aligned} \tag{12}$$

where we used the Maxwell equation $\nabla \times \mathbf{E} + \frac{\partial \mathbf{B}}{\partial t} = 0$ and $\mathbf{E} = -\frac{\partial \mathbf{A}}{\partial t}$ valid in Weyl's temporal gauge with scalar potential set to zero. Thus,

$$\frac{\partial F^{\text{orb}}}{\partial t} + \nabla \cdot \mathcal{J}^{\text{orb}} = 0 \tag{13}$$

with

$$\mathcal{J}^{\text{orb}} = -\mathbf{E} \times \mathbf{M}^{\text{orb}}, \tag{14}$$

as expected.

In the following we discuss several additional formal analogies and similarities between DMI, classical electrodynamics and orbital magnetization. We introduce the tensors $\mathcal{C}(\mathbf{r})$ and $\bar{\mathcal{C}}(\mathbf{r})$ with elements

$$\mathcal{C}_{ij}(\mathbf{r}) = \hat{\mathbf{e}}_i \cdot \left[\hat{\mathbf{n}}(\mathbf{r}) \times \frac{\partial \hat{\mathbf{n}}(\mathbf{r})}{\partial r_j} \right] \tag{15}$$

and

$$\bar{\mathcal{C}}_{ij}(\mathbf{r}) = \frac{\partial \hat{n}_i(\mathbf{r})}{\partial r_j} \tag{16}$$

to quantify the noncollinearity of $\hat{\mathbf{n}}(\mathbf{r})$. \mathcal{C} and $\bar{\mathcal{C}}$ are related through the matrix

$$\mathcal{K}(\hat{\mathbf{n}}) = \begin{pmatrix} 0 & -\hat{n}_3 & \hat{n}_2 \\ \hat{n}_3 & 0 & -\hat{n}_1 \\ -\hat{n}_2 & \hat{n}_1 & 0 \end{pmatrix} \tag{17}$$

as $\mathcal{C} = \mathcal{K} \bar{\mathcal{C}}$. The free energy $F^{\text{DMI}}(\mathbf{r})$ can be expressed in terms of \mathcal{C} and \mathcal{D} as follows:

$$\begin{aligned}
F^{\text{DMI}}(\mathbf{r}) &= \sum_j \mathbf{D}_j(\mathbf{r}) \cdot \left[\hat{\mathbf{n}}(\mathbf{r}) \times \frac{\partial \hat{\mathbf{n}}(\mathbf{r})}{\partial r_j} \right] \\
&= \sum_{ij} \mathcal{D}_{ji}(\mathbf{r}) \hat{\mathbf{e}}_i \cdot \left[\hat{\mathbf{n}}(\mathbf{r}) \times \frac{\partial \hat{\mathbf{n}}(\mathbf{r})}{\partial r_j} \right] \\
&= \sum_{ij} \mathcal{D}_{ji}(\mathbf{r}) \mathcal{C}_{ij}(\mathbf{r}) = \text{Tr}[\mathcal{D}(\mathbf{r}) \mathcal{C}(\mathbf{r})] = \\
&= \text{Tr}[\mathcal{D}(\mathbf{r}) \mathcal{K}(\hat{\mathbf{n}}(\mathbf{r})) \bar{\mathcal{C}}(\mathbf{r})] = \text{Tr}[\bar{\mathcal{D}}(\mathbf{r}) \bar{\mathcal{C}}(\mathbf{r})],
\end{aligned} \tag{18}$$

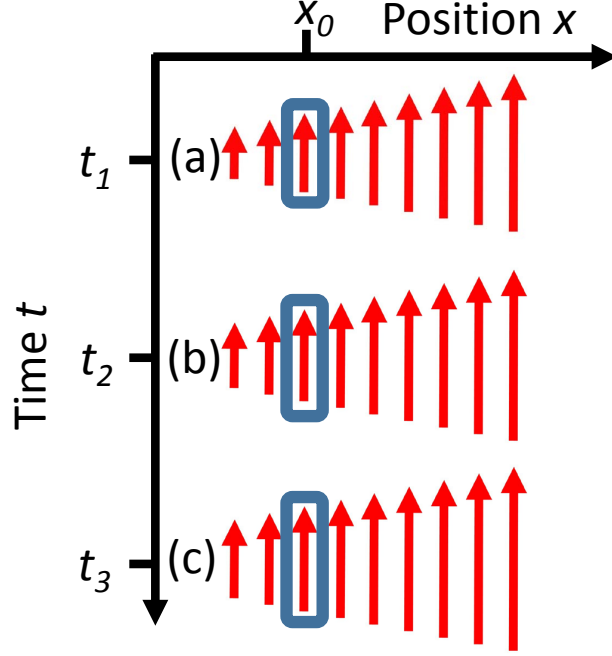


Figure 3. Illustration of a magnetic field ramp that moves into the negative x direction. Arrows represent the magnetic field $B_0(x - wt)\hat{e}_z$ at position x and time t . $B_0(x)$ describes a ramp that increases linearly with x . The magnetic field at position x_0 is highlighted by an oval box. (a) Snapshot at time t_1 . (b) At time t_2 the magnetic field at position x_0 has increased because the ramp has moved to the left since t_1 . Consequently, also the energy density $F_0^{\text{orb}}(x_0 - wt_2)$ is now different. (c) At time t_3 the magnetic field at position x_0 has increased further.

where we defined $\bar{\mathcal{D}} = \mathcal{D}\mathcal{H}$. Similarly, \mathcal{J}^{DMI} in (7) can be expressed in terms of $\bar{\mathcal{D}}$ as

$$\mathcal{J}^{\text{DMI}} = -\mathcal{D}\left(\hat{\mathbf{n}} \times \frac{\partial \hat{\mathbf{n}}}{\partial t}\right) = -\bar{\mathcal{D}}\frac{\partial \hat{\mathbf{n}}}{\partial t}. \quad (19)$$

The energy density $F^{\text{orb}} = -\mathbf{M}^{\text{orb}} \cdot (\nabla \times \mathbf{A})$ in (9) involves the curl of the vector potential \mathbf{A} , while the material-dependent part of the Poynting vector, i.e., $\mathcal{J}^{\text{orb}} = -\mathbf{E} \times \mathbf{M}^{\text{orb}} = \frac{\partial \mathbf{A}}{\partial t} \times \mathbf{M}^{\text{orb}}$, involves the time-derivative of \mathbf{A} . Similarly, the spatial derivatives $\partial \hat{\mathbf{n}} / \partial r_i$ enter F^{DMI} in (18) via the tensor $\bar{\mathcal{C}}$ while the temporal derivative $\partial \hat{\mathbf{n}} / \partial t$ enters \mathcal{J}^{DMI} in (19). Thus, in the theory of DMI the magnetization direction $\hat{\mathbf{n}}$ plays the role of an effective vector potential.

The curl of orbital magnetization constitutes a bound current $\mathbf{J}^{\text{mag}} = \nabla \times \mathbf{M}^{\text{orb}}$ that does not contribute to electronic transport. Hence it needs to be subtracted from the linear response electric current driven by gradients in temperature or chemical potential in order to obtain the measurable electric current [23]. Similarly, the spatial derivatives $\tau_j^{\text{bound}} = \sum_i \frac{\partial}{\partial r_i} \mathcal{D}_{ij} = \nabla \cdot [\mathcal{D}\hat{e}_j]$ that result from the presence of gradients in temperature or chemical potential constitute torques that are not measurable and need to be subtracted from the total linear response to temperature or chemical potential gradients in order to obtain the measurable torque [22]. Table 1 summarizes the formal analogies and similarities between the orbital magnetization and DMI.

Table 1. Formal analogies between the theories of orbital magnetization (OM) and Dzyaloshinskii-Moriya interaction (DMI). The vector potential \mathbf{A} is assumed to satisfy Weyl's temporal gauge, hence the scalar potential is set to zero.

	OM	DMI
'vector potential'	\mathbf{A}	$\hat{\mathbf{n}}$
'magnetic' field	$\mathbf{B} = \nabla \times \mathbf{A}$	$\bar{\mathcal{C}}_{ij} = \frac{\partial \hat{n}_i}{\partial r_j}$
energy density	$F^{\text{orb}} = -\mathbf{M}^{\text{orb}} \cdot \mathbf{B}$	$F^{\text{DMI}} = \text{Tr}[\bar{\mathcal{G}}\bar{\mathcal{C}}]$
'electric' field	$\mathbf{E} = -\frac{\partial \mathbf{A}}{\partial t}$	$\frac{\partial \hat{\mathbf{n}}}{\partial t}$
energy current	$\mathcal{J}^{\text{orb}} = -\mathbf{M}^{\text{orb}} \times \frac{\partial \mathbf{A}}{\partial t}$	$\mathcal{J}^{\text{DMI}} = -\bar{\mathcal{G}} \frac{\partial \hat{\mathbf{n}}}{\partial t}$
bound property	$\mathbf{J}^{\text{mag}} = \nabla \times \mathbf{M}^{\text{orb}}$	$\tau_j^{\text{bound}} = \nabla \cdot [\mathcal{G}\hat{e}_j]$

3. Inverse thermal spin-orbit torque (ITSOT)

In ferromagnets with broken inversion symmetry and SOI, a gradient in temperature T leads to a torque $\boldsymbol{\tau}$ on the magnetization, the so-called thermal spin-orbit torque (TSOT) [22, 21]:

$$\boldsymbol{\tau} = -\boldsymbol{\beta} \nabla T. \quad (20)$$

The inverse thermal spin-orbit torque (ITSOT) consists in the generation of heat current by magnetization dynamics in ferromagnets with broken inversion symmetry and SOI. The effect of magnetization dynamics can be described by the time-dependent perturbation δH to the Hamiltonian H [16]

$$\delta H = \frac{\sin(\omega t)}{\omega} \left[\hat{\mathbf{n}} \times \frac{\partial \hat{\mathbf{n}}}{\partial t} \right] \cdot \boldsymbol{\mathcal{T}}, \quad (21)$$

where $\boldsymbol{\mathcal{T}}(\mathbf{r}) = \mathbf{m} \times \hat{\mathbf{n}} \Omega^{\text{xc}}(\mathbf{r})$ is the torque operator. $\Omega^{\text{xc}}(\mathbf{r}) = \frac{1}{2\mu_{\text{B}}} [V_{\text{minority}}^{\text{eff}}(\mathbf{r}) - V_{\text{majority}}^{\text{eff}}(\mathbf{r})]$ is the exchange field, i.e., the difference between the potentials of minority and majority electrons. $\mathbf{m} = -\mu_{\text{B}} \boldsymbol{\sigma}$ is the spin magnetic moment operator, μ_{B} is the Bohr magneton and $\boldsymbol{\sigma} = (\sigma_x, \sigma_y, \sigma_z)^{\text{T}}$ is the vector of Pauli spin matrices. The energy current \mathcal{J}^E driven by magnetization dynamics is thus given by

$$\mathcal{J}^E = -\mathcal{B}(\hat{\mathbf{n}}) \left[\hat{\mathbf{n}} \times \frac{\partial \hat{\mathbf{n}}}{\partial t} \right], \quad (22)$$

where the tensor \mathcal{B} with elements

$$\mathcal{B}_{ij}(\hat{\mathbf{n}}) = \lim_{\omega \rightarrow 0} \frac{\text{Im} G_{\mathcal{J}_i^E \mathcal{T}_j}^{\text{R}}(\hbar\omega, \hat{\mathbf{n}})}{\hbar\omega} \quad (23)$$

describes the Kubo linear response of the energy current operator

$$\mathcal{J}^E = \frac{1}{2V} [(H - \mu)\mathbf{v} + \mathbf{v}(H - \mu)] \quad (24)$$

to magnetization dynamics. μ is the chemical potential, \mathbf{v} is the velocity operator and the retarded energy-current torque correlation-function is given by

$$G_{\mathcal{J}_i^E, \mathcal{T}_j}^{\text{R}}(\hbar\omega, \hat{\mathbf{n}}) = -i \int_0^{\infty} dt e^{i\omega t} \langle [\mathcal{J}_i^E(t), \mathcal{T}_j(0)]_- \rangle. \quad (25)$$

In (23) we take the limit frequency $\omega \rightarrow 0$, which is justified when the frequency is small compared to the inverse lifetime of electronic states, which is satisfied for magnetic bilayers at room temperature and frequency $\omega/(2\pi)$ in the GHz range.

Within the independent particle approximation (23) becomes $\mathcal{B}_{ij} = \mathcal{B}_{ij}^{\text{I(a)}} + \mathcal{B}_{ij}^{\text{I(b)}} + \mathcal{B}_{ij}^{\text{II}}$, with

$$\begin{aligned} \mathcal{B}_{ij}^{\text{I(a)}} &= \frac{1}{h} \int_{-\infty}^{\infty} d\mathcal{E} \frac{df(\mathcal{E})}{d\mathcal{E}} \text{Tr} \langle \mathcal{J}_i^E G^{\text{R}}(\mathcal{E}) \mathcal{T}_j G^{\text{A}}(\mathcal{E}) \rangle \\ \mathcal{B}_{ij}^{\text{I(b)}} &= -\frac{1}{h} \int_{-\infty}^{\infty} d\mathcal{E} \frac{df(\mathcal{E})}{d\mathcal{E}} \text{Re Tr} \langle \mathcal{J}_i^E G^{\text{R}}(\mathcal{E}) \mathcal{T}_j G^{\text{R}}(\mathcal{E}) \rangle \\ \mathcal{B}_{ij}^{\text{II}} &= -\frac{1}{h} \int_{-\infty}^{\infty} d\mathcal{E} f(\mathcal{E}) \text{Re Tr} \left\langle \mathcal{J}_i^E G^{\text{R}}(\mathcal{E}) \mathcal{T}_j \frac{dG^{\text{R}}(\mathcal{E})}{d\mathcal{E}} \right. \\ &\quad \left. - \mathcal{J}_i^E \frac{dG^{\text{R}}(\mathcal{E})}{d\mathcal{E}} \mathcal{T}_j G^{\text{R}}(\mathcal{E}) \right\rangle, \end{aligned} \quad (26)$$

where $G^{\text{R}}(\mathcal{E})$ and $G^{\text{A}}(\mathcal{E})$ are the retarded and advanced single-particle Green functions, respectively. $f(\mathcal{E})$ is the Fermi function. \mathcal{B} contains scattering-independent intrinsic contributions and, in the presence of disorder, additional disorder-driven contributions. The intrinsic Berry-curvature contribution is given by

$$\begin{aligned} \mathcal{B}_{ij}^{\text{int}} &= \frac{2\hbar}{\mathcal{N}} \sum_{\mathbf{k}n} \sum_{m \neq n} f_{\mathbf{k}n} \text{Im} \frac{\langle \psi_{\mathbf{k}n} | \mathcal{T}_j | \psi_{\mathbf{k}m} \rangle \langle \psi_{\mathbf{k}m} | \mathcal{J}_i^E | \psi_{\mathbf{k}n} \rangle}{(\mathcal{E}_{\mathbf{k}m} - \mathcal{E}_{\mathbf{k}n})^2} \\ &= \frac{1}{\mathcal{N}V} \sum_{\mathbf{k}n} f_{\mathbf{k}n} [A_{\mathbf{k}nji} - (\mathcal{E}_{\mathbf{k}n} - \mu) B_{\mathbf{k}nji}], \end{aligned} \quad (27)$$

where

$$A_{\mathbf{k}nij} = \hbar \sum_{m \neq n} \text{Im} \left[\frac{\langle \psi_{\mathbf{k}n} | \mathcal{T}_i | \psi_{\mathbf{k}m} \rangle \langle \psi_{\mathbf{k}m} | v_j | \psi_{\mathbf{k}n} \rangle}{\mathcal{E}_{\mathbf{k}m} - \mathcal{E}_{\mathbf{k}n}} \right] \quad (28)$$

and

$$B_{\mathbf{k}nij} = -2\hbar \sum_{m \neq n} \text{Im} \left[\frac{\langle \psi_{\mathbf{k}n} | \mathcal{T}_i | \psi_{\mathbf{k}m} \rangle \langle \psi_{\mathbf{k}m} | v_j | \psi_{\mathbf{k}n} \rangle}{(\mathcal{E}_{\mathbf{k}m} - \mathcal{E}_{\mathbf{k}n})^2} \right] \quad (29)$$

and $|\psi_{\mathbf{k}n}\rangle$ are the Bloch wavefunctions with corresponding band energies $\mathcal{E}_{\mathbf{k}n}$, $f_{\mathbf{k}n} = f(\mathcal{E}_{\mathbf{k}n})$, and \mathcal{N} is the number of \mathbf{k} points.

As discussed in section 2 we subtract \mathcal{J}^{DMI} ((7)) from \mathcal{J}^E in order to obtain the heat current \mathcal{J}^{Q} :

$$\mathcal{J}^{\text{Q}} = \mathcal{J}^E - \mathcal{J}^{\text{DMI}} = -\tilde{\beta} \left[\hat{\mathbf{n}} \times \frac{\partial \hat{\mathbf{n}}}{\partial t} \right], \quad (30)$$

with

$$\tilde{\beta} = \mathcal{B} - \mathcal{D}. \quad (31)$$

Inserting the Berry-curvature expression of DMI [22, 28]

$$\mathcal{D}_{ij} = \frac{1}{\mathcal{N}V} \sum_{\mathbf{kn}} \left\{ f_{\mathbf{kn}} A_{\mathbf{kn}ji} + \frac{1}{\beta} \ln [1 + e^{-\beta(\mathcal{E}_{\mathbf{kn}} - \mu)}] B_{\mathbf{kn}ji} \right\}, \quad (32)$$

we obtain for the intrinsic contribution

$$\begin{aligned} \tilde{\beta}_{ij}^{\text{int}} &= \mathcal{B}_{ij}^{\text{int}} - \mathcal{D}_{ij} = \\ &= \frac{1}{\mathcal{N}V} \sum_{\mathbf{kn}} \left\{ f_{\mathbf{kn}} [A_{\mathbf{kn}ji} - (\mathcal{E}_{\mathbf{kn}} - \mu) B_{\mathbf{kn}ji}] \right. \\ &\quad \left. - \left[f_{\mathbf{kn}} A_{\mathbf{kn}ji} + \frac{1}{\beta} \ln [1 + e^{-\beta(\mathcal{E}_{\mathbf{kn}} - \mu)}] B_{\mathbf{kn}ji} \right] \right\} \\ &= -\frac{1}{\mathcal{N}V} \sum_{\mathbf{kn}} B_{\mathbf{kn}ji} \left\{ f_{\mathbf{kn}} (\mathcal{E}_{\mathbf{kn}} - \mu) + \right. \\ &\quad \left. + \frac{1}{\beta} \ln [1 + e^{-\beta(\mathcal{E}_{\mathbf{kn}} - \mu)}] \right\}, \end{aligned} \quad (33)$$

where $\beta = (k_B T)^{-1}$. Using

$$\begin{aligned} f_{\mathbf{kn}} (\mathcal{E}_{\mathbf{kn}} - \mu) + \frac{1}{\beta} \ln [1 + e^{-\beta(\mathcal{E}_{\mathbf{kn}} - \mu)}] &= \\ &= -\int_{-\infty}^{\mu} d\mathcal{E} f'(\mathcal{E}_{\mathbf{kn}} + \mu - \mathcal{E})(\mathcal{E}_{\mathbf{kn}} - \mathcal{E}) = \\ &= -\int_{-\infty}^{\mu} d\mathcal{E} \int_{-\infty}^{\infty} d\mathcal{E}' f'(\mathcal{E}' + \mu - \mathcal{E})(\mathcal{E}' - \mathcal{E}) \delta(\mathcal{E}' - \mathcal{E}_{\mathbf{kn}}) = \\ &= -\int_{-\infty}^{\infty} d\mathcal{E}' f'(\mathcal{E}')(\mathcal{E}' - \mu) \Theta(\mathcal{E}' - \mathcal{E}_{\mathbf{kn}}), \end{aligned} \quad (34)$$

where Θ is the Heaviside unit step function, we can rewrite (33) as

$$\tilde{\beta}_{ij}^{\text{int}}(\hat{\mathbf{n}}) = -\frac{1}{eV} \int_{-\infty}^{\infty} d\mathcal{E} f'(\mathcal{E})(\mathcal{E} - \mu) t_{ji}^{\text{int}}(\hat{\mathbf{n}}, \mathcal{E}). \quad (35)$$

Here,

$$t_{ij}^{\text{int}}(\hat{\mathbf{n}}, \mathcal{E}) = -\frac{e}{\mathcal{N}} \sum_{\mathbf{kn}} \Theta(\mathcal{E} - \mathcal{E}_{\mathbf{kn}}) B_{\mathbf{kn}ij} \quad (36)$$

is the intrinsic SOT torque tensor [16, 22] at zero temperature as a function of Fermi energy \mathcal{E} and $e = |e|$ is the elementary positive charge.

The intrinsic TSOT and ITSOT are even in magnetization, i.e., $\tilde{\beta}_{ij}^{\text{int}}(\hat{\mathbf{n}}) = \tilde{\beta}_{ij}^{\text{int}}(-\hat{\mathbf{n}})$. (26) contains an additional contribution which is odd in magnetization, i.e., $\tilde{\beta}_{ij}^{\text{odd}}(\hat{\mathbf{n}}) = -\tilde{\beta}_{ij}^{\text{odd}}(-\hat{\mathbf{n}})$, and which is given by

$$\tilde{\beta}_{ij}^{\text{odd}}(\hat{\mathbf{n}}) = \frac{1}{eV} \int_{-\infty}^{\infty} d\mathcal{E} f'(\mathcal{E})(\mathcal{E} - \mu) t_{ji}^{\text{odd}}(\hat{\mathbf{n}}, \mathcal{E}), \quad (37)$$

where $t_{ji}^{\text{odd}}(\hat{\mathbf{n}}, \mathcal{E})$ is the odd contribution to the SOT torkance tensor as a function of Fermi energy [16]. The total $\tilde{\beta}_{ij}(\hat{\mathbf{n}})$ coefficient, i.e., the sum of all contributions, is related to the total torkance $t_{ji}(-\hat{\mathbf{n}}, \mathcal{E})$ for magnetization in $-\hat{\mathbf{n}}$ direction by

$$\tilde{\beta}_{ij}(\hat{\mathbf{n}}) = -\frac{1}{eV} \int_{-\infty}^{\infty} d\mathcal{E} f'(\mathcal{E})(\mathcal{E} - \mu) t_{ji}(-\hat{\mathbf{n}}, \mathcal{E}), \quad (38)$$

which contains (35) and (37) as special cases.

It is instructive to verify that the ITSOT described by (38) is the Onsager-reciprocal of the TSOT ((20)), where [22]

$$\beta_{ij}(\hat{\mathbf{n}}) = \frac{1}{e} \int_{-\infty}^{\infty} d\mathcal{E} f'(\mathcal{E}) \frac{(\mathcal{E} - \mu)}{T} t_{ij}(\hat{\mathbf{n}}, \mathcal{E}). \quad (39)$$

Comparison of (38) and (39) yields

$$\boldsymbol{\beta}(\hat{\mathbf{n}}) = -\frac{V}{T} [\tilde{\boldsymbol{\beta}}(-\hat{\mathbf{n}})]^{\text{T}} \quad (40)$$

and thus

$$\begin{pmatrix} -\mathcal{J}^Q \\ \boldsymbol{\tau}/V \end{pmatrix} = \begin{pmatrix} T\boldsymbol{\lambda}(\hat{\mathbf{n}}) & \tilde{\boldsymbol{\beta}}(\hat{\mathbf{n}}) \\ [\tilde{\boldsymbol{\beta}}(-\hat{\mathbf{n}})]^{\text{T}} & -\boldsymbol{\Lambda}(\hat{\mathbf{n}}) \end{pmatrix} \begin{pmatrix} \frac{\nabla T}{T} \\ \hat{\mathbf{n}} \times \frac{\partial \hat{\mathbf{n}}}{\partial t} \end{pmatrix}, \quad (41)$$

where $\boldsymbol{\lambda}$ is the thermal conductivity tensor and $\boldsymbol{\Lambda}$ describes Gilbert damping and gyromagnetic ratio [18]. As expected, the response matrix

$$\mathcal{A}(\hat{\mathbf{n}}) = \begin{pmatrix} T\boldsymbol{\lambda}(\hat{\mathbf{n}}) & \tilde{\boldsymbol{\beta}}(\hat{\mathbf{n}}) \\ [\tilde{\boldsymbol{\beta}}(-\hat{\mathbf{n}})]^{\text{T}} & -\boldsymbol{\Lambda}(\hat{\mathbf{n}}) \end{pmatrix} \quad (42)$$

satisfies the Onsager symmetry $\mathcal{A}(\hat{\mathbf{n}}) = [\mathcal{A}(-\hat{\mathbf{n}})]^{\text{T}}$.

(38) and (30) are the central result of this section. Together, these two equations provide the recipe to compute the heat current \mathcal{J}^Q driven by magnetization dynamics $\partial \hat{\mathbf{n}} / \partial t$. We discuss applications in section 5.

4. Using the ground-state energy currents to derive expressions for DMI and orbital magnetization

The expression (32) for the DMI-spiralization tensor \mathcal{D} was derived both from semiclassics [28] and static quantum mechanical perturbation theory [22]. Alternatively, the $T = 0$ expression of \mathcal{D} can also be obtained elegantly and easily by invoking the third law of thermodynamics: For $T \rightarrow 0$ the ITSOT must vanish, $\tilde{\boldsymbol{\beta}} \rightarrow 0$, because otherwise we could pump heat at zero temperature and thereby violate Nernst's theorem. Hence, $\mathcal{D} \rightarrow \mathcal{B}$ according to (31). In other words, at $T = 0$ the energy current density \mathcal{J}^E in

(22) is identical to the DMI energy current density $\mathcal{J}^{\text{DMI}} = -\mathcal{D} (\hat{\mathbf{n}} \times \frac{\partial \hat{\mathbf{n}}}{\partial t})$ because the heat current is zero. Thus, at $T = 0$ we obtain from (27)

$$\mathcal{D}_{ij} = \mathcal{B}_{ij}^{\text{int}} = \frac{1}{\mathcal{N}V} \sum_{\mathbf{kn}} f_{\mathbf{kn}} [A_{\mathbf{kn}ji} - (\mathcal{E}_{\mathbf{kn}} - \mu) B_{\mathbf{kn}ji}], \quad (43)$$

which agrees with (32) at $T = 0$.

Similarly, we can derive the $T = 0$ expression of orbital magnetization from the energy current $\mathcal{J}^{\text{orb}} = -\mathbf{E} \times \mathbf{M}^{\text{orb}}$ discussed in (14): For $T \rightarrow 0$ the inverse anomalous Nernst effect (i.e., the generation of a transverse heat current by an applied electric field) has to vanish according to the third law of thermodynamics. Hence, the energy current driven by an applied electric field at $T = 0$ does not contain any heat current and is therefore identical to \mathcal{J}^{orb} . We introduce the tensor \mathcal{R} to describe the linear response of the energy current \mathcal{J} to an applied electric field \mathbf{E} , i.e., $\mathcal{J} = \mathcal{R} \mathbf{E}$. We describe the effect of the electric field by the vector potential $\mathbf{A} = -\mathbf{E} \sin(\omega t)/\omega$ and take the limit $\omega \rightarrow 0$ later. The Hamiltonian density describing the interaction between electric current density \mathbf{J} and vector potential is $-\mathbf{J} \cdot \mathbf{A}$, from which we obtain the time-dependent perturbation

$$\delta H = -\frac{\sin(\omega t)}{\omega} e \mathbf{E} \cdot \mathbf{v}. \quad (44)$$

Introducing the retarded energy-current velocity correlation-function

$$G_{\mathcal{J}_i^E, v_j}^{\text{R}}(\hbar\omega) = -i \int_0^{\infty} dt e^{i\omega t} \langle [\mathcal{J}_i^E(t), v_j(0)]_- \rangle \quad (45)$$

we can write the elements of the tensor \mathcal{R} as

$$\mathcal{R}_{ij} = e \lim_{\omega \rightarrow 0} \frac{\text{Im} G_{\mathcal{J}_i^E, v_j}^{\text{R}}(\hbar\omega)}{\hbar\omega}. \quad (46)$$

This allows us to determine \mathcal{J}^{orb} as $\mathcal{J}^{\text{orb}} = \mathcal{R}^{\text{int}} \mathbf{E}$, where the intrinsic Berry-curvature contribution to the response tensor \mathcal{R} is given by

$$\begin{aligned} \mathcal{R}_{ij}^{\text{int}} &= -\frac{2e\hbar}{\mathcal{N}} \sum_{\mathbf{kn}} f_{\mathbf{kn}} \sum_{m \neq n} \text{Im} \frac{\langle u_{\mathbf{kn}} | \mathcal{J}_i^E | u_{\mathbf{km}} \rangle \langle u_{\mathbf{km}} | v_j | u_{\mathbf{kn}} \rangle}{(\mathcal{E}_{\mathbf{km}} - \mathcal{E}_{\mathbf{kn}})^2} \\ &= \frac{1}{\mathcal{N}V} \sum_{\mathbf{kn}} f_{\mathbf{kn}} [\mathcal{M}_{\mathbf{kn}ij} - (\mathcal{E}_{\mathbf{kn}} - \mu) \mathcal{N}_{\mathbf{kn}ij}], \end{aligned} \quad (47)$$

with

$$\mathcal{M}_{\mathbf{kn}ij} = e\hbar \sum_{m \neq n} \text{Im} \frac{\langle u_{\mathbf{kn}} | v_i | u_{\mathbf{km}} \rangle \langle u_{\mathbf{km}} | v_j | u_{\mathbf{kn}} \rangle}{\mathcal{E}_{\mathbf{kn}} - \mathcal{E}_{\mathbf{km}}} \quad (48)$$

and

$$\mathcal{N}_{\mathbf{kn}ij} = 2e\hbar \sum_{m \neq n} \text{Im} \frac{\langle u_{\mathbf{kn}} | v_i | u_{\mathbf{km}} \rangle \langle u_{\mathbf{km}} | v_j | u_{\mathbf{kn}} \rangle}{(\mathcal{E}_{\mathbf{km}} - \mathcal{E}_{\mathbf{kn}})^2}. \quad (49)$$

From $\mathbf{M}^{\text{orb}} \times \mathbf{E} = \mathcal{R}^{\text{int}} \mathbf{E}$ we obtain

$$\mathbf{M}^{\text{orb}} = -\frac{1}{2} \hat{e}_k \epsilon_{kij} \mathcal{R}_{ij}^{\text{int}}. \quad (50)$$

It is straightforward to verify that \mathbf{M}^{orb} given by (50) agrees to the $T = 0$ expressions for orbital magnetization derived from quantum mechanical perturbation theory [33], from semiclassics [23], and within the Wannier representation [34, 35].

Combining the third law of thermodynamics with the continuity equations (8) and (13) provides thus an elegant way to derive expressions for \mathcal{D} and \mathbf{M}^{orb} at $T = 0$. We can extend these derivations to $T > 0$ if we postulate that the linear response to thermal gradients is described by Mott-like expressions. In the case of the TSOT this Mott-like expression is (39), while it is [23, 36, 37]

$$\alpha_{xy} = \frac{1}{e} \int_{-\infty}^{\infty} d\mathcal{E} f'(\mathcal{E}) \frac{\mathcal{E} - \mu}{T} \sigma_{xy}(\mathcal{E}) \quad (51)$$

in the case of the anomalous Nernst effect, where $\sigma_{xy}(\mathcal{E})$ is the zero-temperature anomalous Hall conductivity as a function of Fermi energy \mathcal{E} and the anomalous Nernst current due to a temperature gradient in y direction is $j_x = -\alpha_{xy} \partial T / \partial y$. While (39) and (51) were, respectively, derived in the previous section and in [23], we now instead consider it an axiom that within the range of validity of the independent particle approximation the linear response to thermal gradients is always described by Mott-like expressions. Thereby, the derivation in the present section becomes independent from the derivation in the preceding section. Applying the Onsager reciprocity principle to (39) and (51) we find that the ITSOT and the inverse anomalous Nernst effect are, respectively, described by (38) and by

$$\mathcal{J}_y^Q = T \alpha_{xy} E_x. \quad (52)$$

Employing the general identity (34) (but in contrast to section 3 we now use it backwards) we obtain

$$\begin{aligned} \tilde{\beta}_{ij}^{\text{int}} = & -\frac{1}{\mathcal{N}V} \sum_{\mathbf{kn}} B_{\mathbf{kn}ji} \left\{ f_{\mathbf{kn}}(\mathcal{E}_{\mathbf{kn}} - \mu) + \right. \\ & \left. + \frac{1}{\beta} \ln [1 + e^{-\beta(\mathcal{E}_{\mathbf{kn}} - \mu)}] \right\} \end{aligned} \quad (53)$$

from (35) and, similarly, (52) can be written as

$$\begin{aligned} \mathcal{J}_y^Q = & -\frac{1}{\mathcal{N}V} \sum_{\mathbf{kn}} \mathcal{N}_{\mathbf{kn}yx} \left\{ f_{\mathbf{kn}}(\mathcal{E}_{\mathbf{kn}} - \mu) + \right. \\ & \left. + \frac{1}{\beta} \ln [1 + e^{-\beta(\mathcal{E}_{\mathbf{kn}} - \mu)}] \right\} E_x. \end{aligned} \quad (54)$$

The finite- T expressions of \mathcal{D} and \mathbf{M}^{orb} are now easily obtained, respectively, by subtracting the ITSOT heat current given by (53) from the energy current (27) and

by subtracting the heat current (54) from $\mathcal{J}_y = \mathcal{R}_{yx}^{\text{int}} E_x$. This leads to (32) for the DMI spiralization tensor and to

$$M_z^{\text{orb}} = \frac{1}{\mathcal{N}V} \sum_{kn} f_{kn} \left\{ \mathcal{M}_{knyx} + \frac{1}{\beta} \mathcal{N}_{knyx} \ln[1 + e^{-\beta(\varepsilon_{kn} - \mu)}] \right\} \quad (55)$$

for the orbital magnetization. (55) agrees to the finite- T expressions of M_z^{orb} derived elsewhere [33, 23].

5. Ab-initio calculations

We investigate TSOT and ITSOT in a Mn/W(001) magnetic bilayer composed of one monolayer of Mn deposited on 9 layers of W(001). The ground state of this system is magnetically noncollinear and can be described by the cycloidal spin spiral (2) [31]. Based on phenomenological grounds [38, 19] we can expand torkance as well as TSOT and ITSOT coefficients locally at a given point in space in terms of $\hat{\mathbf{n}}$ and $\bar{\mathcal{E}}$:

$$\begin{aligned} t_{ij}(\hat{\mathbf{n}}, \bar{\mathcal{E}}) &= \sum_k t_{ijk}^{(1,0)} \hat{n}_k + \sum_{kl} t_{ijkl}^{(0,1)} \bar{\mathcal{E}}_{kl} + \\ &+ \sum_{klm} t_{ijklm}^{(1,1)} \hat{n}_k \bar{\mathcal{E}}_{lm} + \sum_k t_{ijkl}^{(2,0)} \hat{n}_k \hat{n}_l + \dots \end{aligned} \quad (56)$$

The coefficients $t_{ijk}^{(1,0)}$, $t_{ijkl}^{(0,1)}$, $t_{ijklm}^{(1,1)}$, ... in this expansion can be extracted from magnetically collinear calculations. Analogous expansions of the TSOT and ITSOT coefficients are of the same form. Here, we consider only $t_{ijk}^{(1,0)}$ and $t_{ijkl}^{(2,0)}$, which give rise to the following contribution to the torque $\boldsymbol{\tau}$:

$$\begin{aligned} \boldsymbol{\tau} &= t_{xx}^{\text{odd}}(\hat{\mathbf{e}}_z) \hat{\mathbf{n}} \times (\mathbf{E} \times \hat{\mathbf{e}}_z) + \\ &+ t_{yx}^{\text{even}}(\hat{\mathbf{e}}_z) \hat{\mathbf{n}} \times [\hat{\mathbf{n}} \times (\mathbf{E} \times \hat{\mathbf{e}}_z)], \end{aligned} \quad (57)$$

where we used that for magnetization direction $\hat{\mathbf{n}}$ along z it follows from symmetry considerations that $t_{xx} = t_{yy}$, $t_{xy} = -t_{yx}$, $t_{xx}^{\text{even}} = 0$ and $t_{yx}^{\text{odd}} = 0$. The SOT in this system has already been discussed by us [16]. In order to obtain TSOT and ITSOT, we calculate the torkance for the magnetically collinear ferromagnetic state with magnetization direction $\hat{\mathbf{n}}$ set along z as a function of Fermi energy and use (39) and (38) to determine the TSOT and ITSOT coefficients β and $\tilde{\beta}$, respectively. Computational details of the density-functional theory calculation of the electronic structure as well as technical details of the torkance calculation are given in [16]. The torkance calculation is performed with the help of Wannier functions [39, 40] and a quasiparticle broadening of $\Gamma = 25$ meV is applied.

Due to symmetry it suffices to discuss the TSOT coefficients β_{yx}^{even} and β_{xx}^{odd} , which are shown in Figure 4 as a function of temperature. For small temperatures we find $\beta_{ij} \propto T$ as expected from

$$\beta_{ij} \simeq -\frac{\pi^2 k_B^2 T}{3e} \frac{\partial t_{ij}}{\partial \mu}, \quad (58)$$

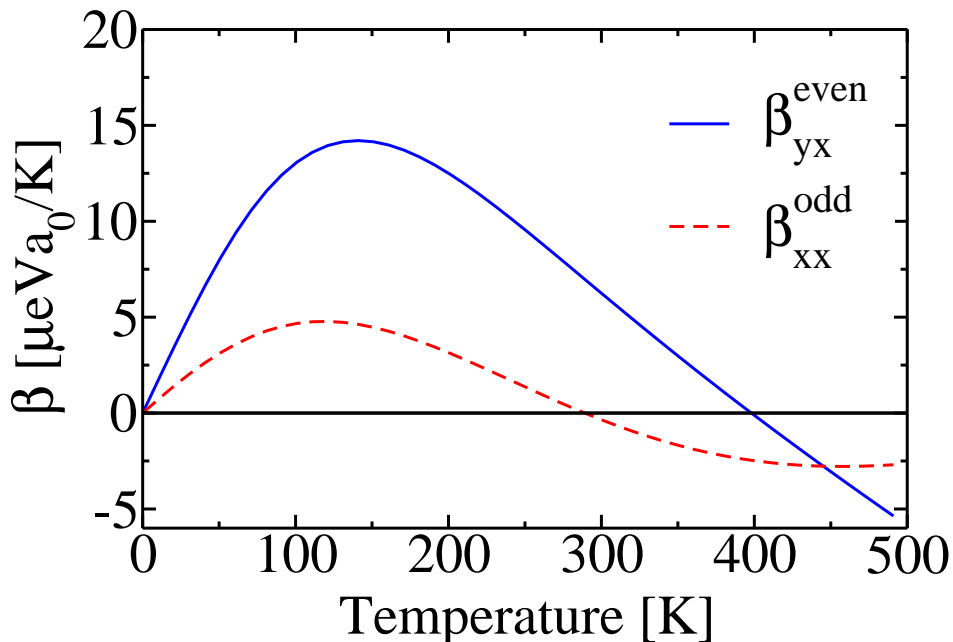


Figure 4. Thermal torkance β vs. temperature of a Mn/W(001) magnetic bilayer for magnetization in z direction. Solid line: Even component β_{yx}^{even} of the thermal torkance. Dashed line: Odd component β_{xx}^{odd} of the thermal torkance. β is plotted in units of $\mu\text{eV}a_0/K = 8.478 \times 10^{-36} \text{Jm/K}$, where a_0 is Bohr's radius.

which is obtained from (39) using the Sommerfeld expansion. Slightly above 100K both β_{yx}^{even} and β_{xx}^{odd} stop following the linear behavior of the low temperature expansion (58): After reaching a maximum both β_{yx}^{even} and β_{xx}^{odd} decrease and finally change sign. At $T = 300\text{K}$ the thermal torkances are $\beta_{yx}^{\text{even}} = 5.24 \times 10^{-35} \text{Jm/K}$ and $\beta_{xx}^{\text{odd}} = -3.21 \times 10^{-36} \text{Jm/K}$. Thermal torkances of comparable magnitude have been determined in calculations on FePt/Pt magnetic bilayers [21].

Using (40) and the volume of the unit cell of $V = 1.58 \times 10^{-28} \text{m}^3$ to convert the TSOT coefficients into ITSOT coefficients, we obtain $\tilde{\beta}_{yx}^{\text{even}} = -99.49 \mu\text{J/m}^2$ and $\tilde{\beta}_{xx}^{\text{odd}} = -6.09 \mu\text{J/m}^2$ at $T = 300\text{K}$. When the magnetization precesses around the z axis in ferromagnetic resonance (this situation is sketched in Figure 1d) with frequency ω and cone angle θ according to

$$\hat{\mathbf{n}}(t) = [\sin(\theta) \cos(\omega t), \sin(\theta) \sin(\omega t), \cos(\theta)]^T, \quad (59)$$

the following ITSOT heat current is obtained from (30) in the limit of small θ :

$$\begin{aligned} \mathcal{J}_x^Q &= \omega\theta \left[\tilde{\beta}_{xx}^{\text{odd}} \cos(\omega t) - \tilde{\beta}_{yx}^{\text{even}} \sin(\omega t) \right] \\ \mathcal{J}_y^Q &= \omega\theta \left[\tilde{\beta}_{yx}^{\text{even}} \cos(\omega t) + \tilde{\beta}_{xx}^{\text{odd}} \sin(\omega t) \right], \end{aligned} \quad (60)$$

where we made use of $\tilde{\beta}_{xx} = \tilde{\beta}_{yy} = \tilde{\beta}_{xx}^{\text{odd}}$ and $-\tilde{\beta}_{xy} = \tilde{\beta}_{yx} = \tilde{\beta}_{yx}^{\text{even}}$, which follows from symmetry considerations. Using the ITSOT coefficients $\tilde{\beta}_{yx}^{\text{even}}$ and $\tilde{\beta}_{xx}^{\text{odd}}$ determined above

at $T = 300\text{K}$ we can determine the amplitudes of \mathcal{J}_x^Q and \mathcal{J}_y^Q . Assuming a cone angle of 1° and a frequency of $\omega = 2\pi \cdot 5\text{GHz}$ we find that the amplitude of the oscillating heat current density \mathcal{J}_x^Q is

$$\omega\theta\sqrt{\left(\tilde{\beta}_{yx}^{\text{even}}\right)^2 + \left(\tilde{\beta}_{xx}^{\text{odd}}\right)^2} \approx 55\frac{\text{kW}}{\text{m}^2}. \quad (61)$$

The heat current density \mathcal{J}_y^Q has the same amplitude. We can use the thermal conductivity of bulk W of $\lambda_{xx}=174\text{ W}/(\text{Km})$ [41] at $T=300\text{ K}$ to estimate the temperature gradient needed to drive a heat current of this magnitude: $(55\text{kW}/\text{m}^2)/\lambda_{xx}=316\text{ K}/\text{m}$. The thickness of the Mn/W(001) film is 1.58 nm . The amplitude of the heat current per length flowing in x direction is thus $55\text{ kW}/\text{m}^2 \cdot 1.58\text{ nm} \approx 87\mu\text{W}/\text{m}$. These estimates suggest that \mathcal{J}^Q is measurable in ferromagnetic resonance experiments.

According to (60) the heat current can be made larger by increasing the cone angle. However, in ferromagnetic resonance experiments the cone angle θ is small. Therefore, we estimate the heat current driven by a flat cycloidal spin spiral that moves with velocity w in x direction. Its magnetization direction is given by

$$\hat{\mathbf{n}}_c(\mathbf{r}, t) = \hat{\mathbf{n}}_c(x, t) = \begin{pmatrix} \sin(qx - wt) \\ 0 \\ \cos(qx - wt) \end{pmatrix}. \quad (62)$$

With $\hat{\mathbf{n}}_c(\mathbf{r}, t) \times \partial\hat{\mathbf{n}}_c(\mathbf{r}, t)/\partial t = wq\hat{\mathbf{e}}_y$ we get

$$\mathcal{J}_x^Q = -\tilde{\beta}_{xy}^{\text{even}}wq \quad (63)$$

from (30), i.e., a constant-in-time heat current in x direction. Using $\tilde{\beta}_{xy}^{\text{even}} = 99.49\mu\text{J}/\text{m}^2$ determined above and a spin-spiral wavelength of 2.3nm [31] we obtain a heat current density of $\mathcal{J}_x^Q = -270\text{kW}/\text{m}^2$ for a spin spiral moving with a speed of $w=1\text{ms}^{-1}$. This estimate suggests that fast domain walls moving at a speed of the order of 100ms^{-1} drive significant heat currents that correspond to temperature gradients of the order of $0.1\text{K}/(\mu\text{m})$.

6. Summary

Magnetization dynamics drives heat currents in magnets with broken inversion symmetry and SOI. This effect is the inverse of the thermal spin-orbit torque. We use the Kubo linear-response formalism to derive equations suitable to calculate the inverse thermal spin-orbit torque (ITSOT) from first principles. We find that a ground-state energy current associated with the Dzyaloshinskii-Moriya interaction (DMI) is driven by magnetization dynamics and needs to be subtracted from the linear response

of the energy current in order to extract the heat current. We show that the ground-state energy currents obtained from the Kubo linear-response formalism can also be used to derive expressions for DMI and for orbital magnetization. The ITSOT extends the picture of phenomena associated with the coupling of spin to electrical currents and heat currents in magnets with broken inversion symmetry and SOI. Based on *ab-initio* calculations we estimate the heat currents driven by magnetization precession and moving spin-spirals in Mn/W(001) magnetic bilayers. Our estimates suggest that fast domain walls in magnetic bilayers drive significant heat currents.

Acknowledgments

We gratefully acknowledge computing time on the supercomputers of Jülich Supercomputing Center and RWTH Aachen University as well as financial support from the programme SPP 1538 Spin Caloric Transport of the Deutsche Forschungsgemeinschaft.

- [1] Bauer G E W, Saitoh E and van Wees B J 2012 *Nature materials* **11** 391
- [2] Chico J, Etz C, Bergqvist L, Eriksson O, Fransson J, Delin A and Bergman A 2014 *Phys. Rev. B* **90**(1) 014434
- [3] Yuan Z, Wang S and Xia K 2010 *Solid state communications* **150** 548
- [4] Kim S K and Tserkovnyak Y 2015 *Phys. Rev. B* **92**(2) 020410
- [5] Hatami M, Bauer G E W, Zhang Q and Kelly P J 2007 *Phys. Rev. Lett.* **99**(6) 066603
- [6] Jia X, Xia K and Bauer G E W 2011 *Phys. Rev. Lett.* **107**(17) 176603
- [7] Yu H, Granville S, Yu D P and Ansermet J P 2010 *Phys. Rev. Lett.* **104**(14) 146601
- [8] Leutenantsmeyer J C, Walter M, Zbarsky V, Münzenberg M, Gareev R, Rott K, Thomas A, Reiss G, Peretzki P, Schuhmann H, Seibt M, Czerner M and Heiliger C 2013 *SPIN* **03** 1350002
- [9] Manchon A and Zhang S 2008 *Phys. Rev. B* **78**(21) 212405
- [10] Garate I and MacDonald A H 2009 *Phys. Rev. B* **80**(13) 134403
- [11] Chernyshov A, Overby M, Liu X, Furdyna J K, Lyanda-Geller Y and Rokhinson L P 2009 *Nature Phys.* **5** 656
- [12] Liu L, Lee O J, Gudmundsen T J, Ralph D C and Buhrman R A 2012 *Phys. Rev. Lett.* **109**(9) 096602
- [13] Garello K, Miron I M, Avci C O, Freimuth F, Mokrousov Y, Blügel S, Auffret S, Boule O, Gaudin G and Gambardella P 2013 *Nature Nanotech.* **8** 587
- [14] Haney P M, Lee H W, Lee K J, Manchon A and Stiles M D 2013 *Phys. Rev. B* **87**(17) 174411
- [15] Kurebayashi H, Sinova J, Fang D, Irvine A C, Skinner T D, Wunderlich J, Novak V, Champion R P, Gallagher B L, Vehstedt E K, Zarbo L P, Vyborny K, Ferguson A J and Jungwirth T 2014 *Nature nanotechnology* **9** 211
- [16] Freimuth F, Blügel S and Mokrousov Y 2014 *Phys. Rev. B* **90**(17) 174423
- [17] Manchon A, Koo H C, Nitta J, Frolov S M and Duine R A 2015 *Nature materials* **14** 871
- [18] Freimuth F, Blügel S and Mokrousov Y 2015 *Phys. Rev. B* **92**(6) 064415
- [19] Hals K M D and Brataas A 2015 *Phys. Rev. B* **91**(21) 214401
- [20] Ciccarelli C, Hals K M D, Irvine A, Novak V, Tserkovnyak Y, Kurebayashi H, Brataas A and Ferguson A 2014 *Nature nanotechnology* **10** 50
- [21] Géranton G, Freimuth F, Blügel S and Mokrousov Y 2015 *Phys. Rev. B* **91**(1) 014417
- [22] Freimuth F, Blügel S and Mokrousov Y 2014 *Journal of physics: Condensed matter* **26** 104202
- [23] Xiao D, Yao Y, Fang Z and Niu Q 2006 *Phys. Rev. Lett.* **97**(2) 026603
- [24] Cooper N R, Halperin B I and Ruzin I M 1997 *Phys. Rev. B* **55**(4) 2344
- [25] Qin T, Niu Q and Shi J 2011 *Phys. Rev. Lett.* **107**(23) 236601

- [26] Moriya T 1960 *Phys. Rev.* **120**(1) 91
- [27] Dzyaloshinsky I 1958 *Journal of Physics and Chemistry of Solids* **4** 241
- [28] Freimuth F, Bamler R, Mokrousov Y and Rosch A 2013 *Phys. Rev. B* **88**(21) 214409
- [29] Kovalev A A and GÜngördü U 2015 *epl* **109** 67008
- [30] Manchon A, Ndiaye P B, Moon J H, Lee H W and Lee K J 2014 *Phys. Rev. B* **90**(22) 224403
- [31] Ferriani P, von Bergmann K, Vedmedenko E Y, Heinze S, Bode M, Heide M, Bihlmayer G, Blügel S and Wiesendanger R 2008 *Phys. Rev. Lett.* **101**(2) 027201
- [32] Yang H, Thiaville A, Rohart S, Fert A and Chshiev M 2015 *Phys. Rev. Lett.* **115**(26) 267210
- [33] Shi J, Vignale G, Xiao D and Niu Q 2007 *Phys. Rev. Lett.* **99**(19) 197202
- [34] Thonhauser T, Ceresoli D, Vanderbilt D and Resta R 2005 *Phys. Rev. Lett.* **95**(13) 137205
- [35] Ceresoli D, Thonhauser T, Vanderbilt D and Resta R 2006 *Phys. Rev. B* **74**(2) 024408
- [36] Weischenberg J, Freimuth F, Blügel S and Mokrousov Y 2013 *Phys. Rev. B* **87**(6) 060406
- [37] Wimmer S, Ködderitzsch D and Ebert H 2014 *Phys. Rev. B* **89**(16) 161101
- [38] van der Bijl E and Duine R A 2012 *Phys. Rev. B* **86**(9) 094406
- [39] Mostofi A A, Yates J R, Lee Y S, Souza I, Vanderbilt D and Marzari N 2008 *Computer Physics Communications* **178** 685
- [40] Freimuth F, Mokrousov Y, Wortmann D, Heinze S and Blügel S 2008 *Phys. Rev. B* **78** 035120
- [41] Ho C Y, Powell R W and Liley P E 1972 *Journal of physical and chemical reference data* **1** 279